Characterisation of Adhesive Bonds from Inspection by Laser-Generated Ultrasound

R. Ince[a]; G. E. Thompson[a]; R. J. Dewhurst[a]

[a] Department of Instrumentation and Analytical Science, Corrosion and Protection Centre, University of Manchester Institute of Science and Technology, Manchester, UK

PLEASE SCROLL DOWN FOR ARTICLE

Characterisation of Adhesive Bonds from Inspection by Laser-Generated Ultrasound

R. INCE, G. E. THOMPSON* and R. J. DEWHURST**

*Department of Instrumentation and Analytical Science, *Corrosion and Protection Centre, University of Manchester Institute of Science and Technology, PO Box 88, Manchester, M60 1QD, UK*

Ultrasonic transients with high frequency components have been used to interrogate the bond region of lap-bonded joints. With through-transmission measurements, based on a non-contact laser technique, wave arrival times have been identified in addition to internal reflections within the joint region. This knowledge has led to analysis of wave amplitudes reverberating within the bond, from which the local density of the adhesive has been derived. Furthermore, shear wave signal amplitudes are significantly attenuated for a poorly-bonded joint compared with a well-bonded sample. The data reveal that a laser-ultrasound approach may be used to assess the condition of a lap-bonded joint.

KEY WORDS aluminium bonds; adhesion; ultrasound; laser generation; laser detection; ultrasonic transients; through-transmission measurements; lap joints; local density of adhesive.

INTRODUCTION

Adhesive bonding has been used extensively for many years in aerospace and high technology industries. Adhesives are attractive because they enable stress to be distributed over the entire bond area, therefore avoiding the stress concentrations which occur with mechanical fasteners. This leads to an improved appearance, reduced weight and, in the aerospace industry, fuel savings. The strength of the bonded area is of paramount importance. A fault or defect is defined by Adams *et al.*[1,3] as anything which influences the short or long term strength of a joint.

The objective of any system which examines an adhesive joint must be to obtain a correlation between the strength of the joint and some mechanical, physical or chemical parameter which can be measured readily without causing deterioration of the joint. Thus non-destructive testing (NDT) techniques must be employed, which are considered further in this paper.

There are three basic categories of defect:

**Corresponding author.

(i)   Voids and porosity. These may be located, for example, by using time domain ultrasonics combined with a scanning mechanism to give C-scan presentations, as described by Adams et al.[1] They may also be detected by mechanical impedance measurements detailed by Cawley,[2] thermography tests[3] as well as conventional ultrasound methods used by Hagemaier.[4,5]

(ii) Limited cohesive strength. This may arise from insufficient cure of the adhesive. Measurements to assess cohesive strength have been unsuccessful using thermography, mechanical impedance and coin-tap techniques. It is even difficult to assess using ultrasonic NDT techniques, since the adhesive layer is highly attenuative of ultrasound. However, detection of cohesive strength has been reported by Rose et al.[6] using an ultrasonic oblique incidence technique. In an earlier decade,[7] the Fokker Bond Tester (50–500 kHz) was a commercial instrument which was thought to be capable of providing a correlation with the cohesive strength of an adhesive bond under certain conditions. However, it is now only used by aerospace companies for debond detection.

(iii) Poor adhesive strength. Poor strength between the adhesive and adherend is usually caused by poor, or insufficient, surface preparation, such as improper cleaning.[8] Currently, there is no method of testing for this particular defect using NDT techniques, because it is an interfacial problem involving a very thin layer of material.

Before adhesive bonding can become more widely used and accepted, techniques are required to ensure the quality of the bond. An absolute method for determination of bond quality does not exist. A weak bond, or a bond which is not well joined, is defined as a "disbond" by many authors.[1,2,3,8,11] However, although ultrasonic techniques have been under development for some time, they only deal with sizing of disbonds.[1]

Ultrasonic testing is the most widely used technique for the NDT of bonded joints. Conventional ultrasonic methods used for the testing of cohesive and adhesive strength are summarised below, prior to considering an alternative technique employing laser-generated ultrasound pulses. Such ultrasound, in the form of pulses or transients, is launched into the system with a view to detecting scattering or reflection from internal defects.

Advantages of conventional ultrasound measurements include transducers generating ultrasonic disturbances which are well characterised with regards to frequencies and modes. This may not be true of laser-ultrasound, when laser stimulated thermal expansion, perhaps accompanied by material ablation, creates a disturbance which depends on the properties of the material under investigation. Nevertheless, laser-ultrasound offers sensing areas much smaller (<1 mm^2) than conventional techniques, and potentially very broadband frequency content in ultrasonic disturbances (>100 MHz). Ultrasonic features are sometimes extracted from material interactions which might otherwise be integrated from detection with larger area probes.

The potential of this approach, applied to adhesively-bonded aluminium, is the subject of this paper.

METHODS OF NDE FOR BOND CHARACTERISATION

(a) Pulse-Echo (Reflection) and Through Transmission Methods

Time domain ultrasonics is a method for detection of voids[4,5] etc., and has been used as a method of predicting cohesive strength by Rose *et al.*,[6] amongst others.[9] As a pulse of ultrasound propagates through a bonded region between two materials, a joint for example, part of its energy is reflected at the boundary. The amount of energy reflected depends on the acoustic impedance,[10] z, of the materials on either side of the boundary (Figure 1).

The amplitudes of the reflected and transmitted pulses depend on the reflection, R_{12}, and transmission, T_{12}, coefficients of the materials on either side of the boundary between the two regions where,

$$R_{12} = \frac{z_2 - z_1}{z_2 + z_1} \tag{1}$$

$$T_{12} = 1 + R_{12} \tag{2}$$

In these equations, the impedance of the material in which ultrasound is initially propagating (material 1) is z_1, and z_2 is the impedance of the material 2 on the other side of the boundary. The impedance, z, is the product of the density, ρ, of either material multiplied by the velocity, c, of sound inside the same material. When $z_1 > z_2$, R_{12} is negative and the polarity of the pulse is inverted with respect to the pulse in material 1.
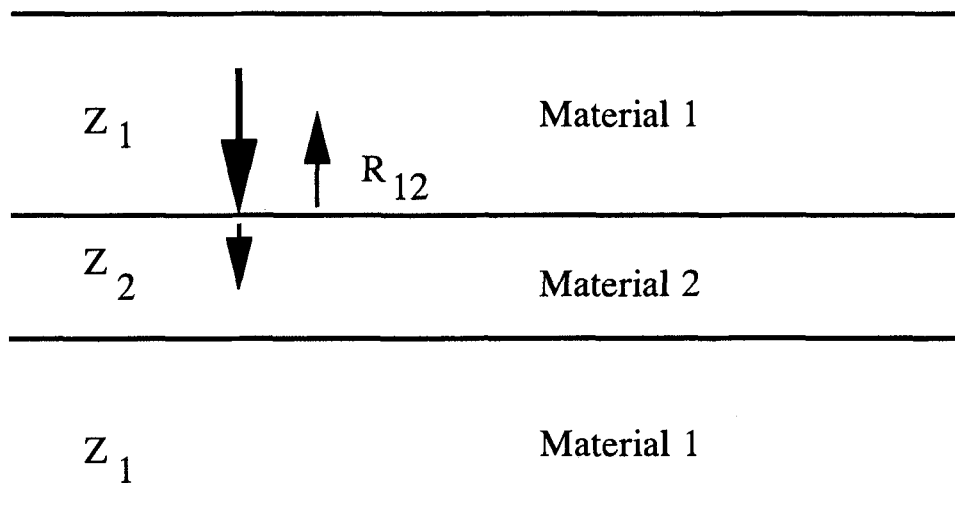

FIGURE 1 Propagation of ultrasound through a bonded region in an aluminium lap-joint, where aluminium is denoted by material 1, and the bond region by material 2.

A defect (*i.e.* an air pocket or an area containing a low density substance) has a low impedance relative to the adhesive; hence, ultrasound is almost totally reflected at the boundary of this defect. Consequently, the signal for through transmission either reduces or disappears when a defect is present, and the reflection coefficient tends to 1.0 (100%). Results by Pilarski and Rose[11] indicate a possible correlation between mechanical strength of a bonded region and the reflection coefficient at the boundary between the adherend and adhesive.

(b) Ultrasonic Spectroscopy

Signals measured by the previous two methods, pulse-echo and through transmission, are analyzed in the frequency domain by performing a Fourier transform.[12] The advantage of this technique is its ability to reveal frequency-dependent features which cannot be identified easily in the time domain. This is meaningful if broadband transducers are used and the excitation is not a tone burst. Furthermore, the detected signals can be processed with various enhancement techniques to improve signal-to-noise ratios, for example using filtering, convolution and correlation techniques.[13] Bonded and un-bonded systems are distinguished from each other by the number and location of the minima and maxima in the reflection/transmission coefficients as functions of frequency. These minima/maxima are the results of interference of the waves within the system; thus, anything which alters the bond conditions will change the spectrum. Pilarski and Rose[11] utilised ultrasonic oblique incidence in interface weakness detection, using a signal feature in the frequency domain. Using a 2 MHz bandwidth, centered around a peak of either 10 MHz or 20 MHz, they found that, in the case of poor adhesion, the frequency signature from a power spectrum of the reflected signal showed a 500 kHz peak frequency increase.

It can be shown that positions of peaks in the frequency spectra are highly sensitive to disbonds, adhesive thickness and adhesive ultrasonic velocity.[14] Disbonds give a different frequency response from normal samples and hence are readily detected.

(c) Leaky Lamb Waves

Here, the wave is not directed at the joint, but it is launched parallel to the surface; measurements then depend on the Lamb wave coupling into the joint as it propagates as a plate wave. Although Lamb waves are presently used for the study of adhesive bonds, interpretation of resultant data is frequently complicated.[15] Several Lamb modes may exist at the same frequency, with velocity dispersion evident. If velocities of the modes are similar, a considerable propagation distance is required for their distinction, and the shape of the response signal varies along the plate surface.

(d) Laser-Generated Ultrasound

In laser-generated ultrasound, a source laser is used to generate ultrasound by releasing short pulses of energy ($\approx$50 mJ) onto a sample surface, with typical laser

pulse durations of 5–40 ns timescale. This causes large power densities to be incident on the surface, the power being dependent on the beam diameter at the focus. Ultrasonic transients having broad-band frequency components[16] are thus generated; these transients contain bulk waves, consisting of compression waves (or longitudinal waves) and transverse waves (or shear waves). In a time-domain analysis, the longitudinal wave arrives first, followed by the broader shear arrival. Laser-generated ultrasound offers high spatial and temporal resolution. The high spatial resolution arises because the source layer may be focused to an area of less than 1 mm^2, giving the possibility of investigating small areas of disbond[1] or contamination.

Laser-generated ultrasound is already an established research technique for examination of sub-surface defects[16] and materials characterisation.[17–19] In this paper, we perform an initial study of laser-ultrasound waveforms obtained from adhesive bonds to examine their potential for the characterisation of bonds.

To take full advantage of laser-ultrasound features, an optical detection system was employed to enable the technique to be fully remote and non-contacting. A continuous wave He-Ne laser monitored the sample surface. Some of the backscattered light, corresponding to one of the brightest speckle points, was analyzed in a Michelson interferometer arrangement. It was this back-scattered light which contained information arising from ultrasound monitored on the sample surface.

EXPERIMENTAL ARRANGEMENT

A pulsed laser source (Nd:YAG), a detector laser (He-Ne) and a Michelson interferometer were used to obtain ultrasonic data from adhesively-bonded aluminium joints supplied by the Bonded Structure Division, Ceiba-Geigy Plc., Duxford, UK. The experimental arrangement is shown in the schematic diagram of Figure 2.

A Q-switched Nd:YAG laser operated at 1.06 μm with a pulse duration of 20 ns, generating an ultrasonic pulse with frequency components in the range 1–50 MHz.[20] Output pulses with ≈30 mJ in energy were focused onto one side of a sample by a converging lens, to produce a small plasma on the surface. Ultrasonic waves were detected on epicentre by a 5 mW He-Ne laser, which formed part of a broadband (2 kHz–130 MHz) Michelson interferometer. Stabilisation of the interferometer was achieved using an electro-mechanical vibrating mirror, driven by a feedback signal from the interferometer output. In this way, compensation for low frequency noise up to 700 Hz was achieved with up to 97% efficiency.[20]

For ultrasonic signal capture, the present system incorporated a 7912 AD Tektronix digitiser, which maintains 512 digitising points on all waveform capture timescales. During the course of experiments, it was found that this feature restricted information on frequency content when operating on timescales greater than 1 μs.

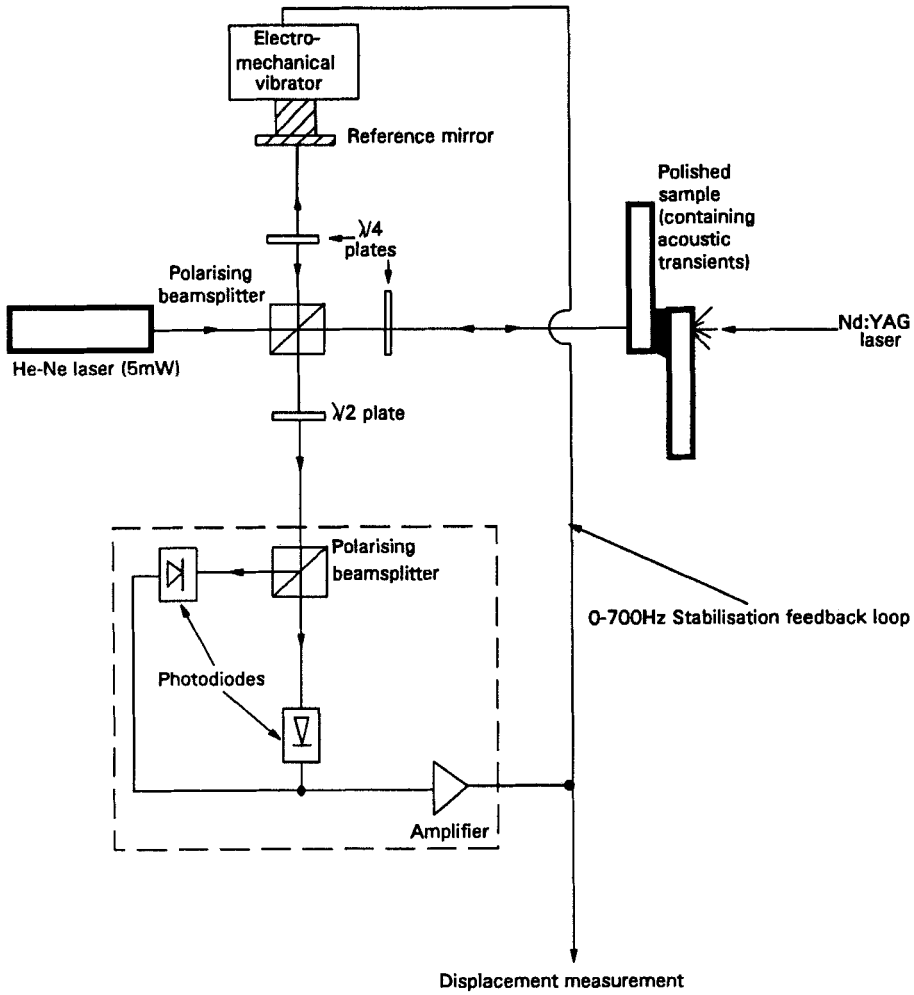Because an interferometer was used in detection, an evaluation of the absolute

FIGURE 2 Michelson interferometer arrangement used for transient signal capture of ultrasonic signals.

magnitude of ultrasonic amplitudes could be made. The calibration equation of the laser interferometer for a small displacement, x, is given by,

$$x = \frac{V\lambda}{4\pi V_o} \tag{3}$$

where V is the output voltage of the detector, λ is the laser wavelength (632.8 nm) and V_o is the peak voltage amplitude when un-stabilised.

Transient sample displacements of a few nanometres occurred, thus representing fractional fringe shifts in the interferometer, where one fringe corresponded to $\lambda/4$ (158.2 nm).
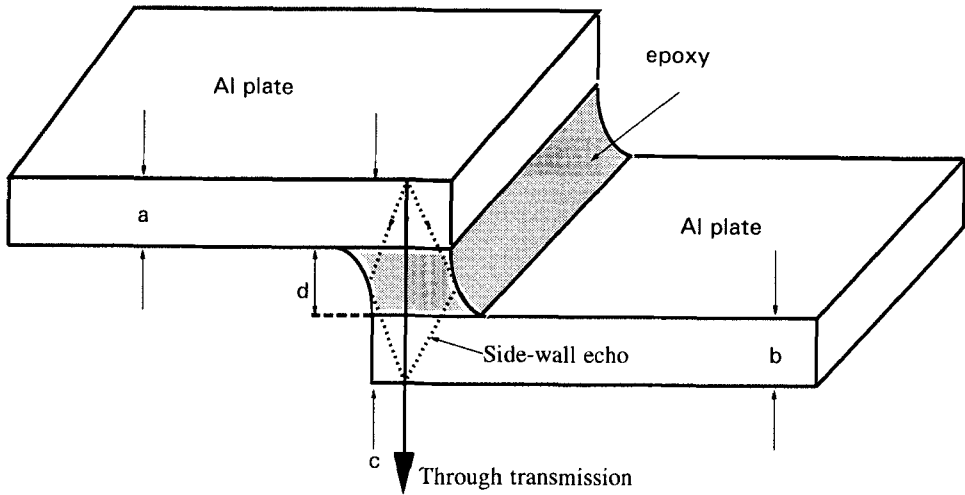
FIGURE 3   Schematic diagram of an aluminium-epoxy-aluminium interface in a single lap joint.

TABLE I
Typical dimensions of thick and thin bonded joints

THICK/mm				THIN/mm			
a	b	c	d*	a	b	c	d**
1.556	1.551	4.568	1.461	1.556	1.553	3.211	0.102

Three sets of aluminium adhesive joints were prepared from aluminium sheet thickness of approximately 1.5 mm. These included:

(i)   thick joints, (produced commercially to acceptable quality standards), where thick refers to an adhesive thickness of 1.46 mm,
(ii) thin joints, where thin refers to an adhesive thickness of 0.102 mm, and
(iii) thin contaminated joints, which were deliberately oil contaminated.

In all cases the aluminium was pre-treated with a chromate-sulphuric acid pickle. Figure 3 is a schematic diagram of a single lap joint used, where a, b, c and d were measured using a micrometer screw gauge to give the dimensions recorded in Table I. The dimensions of the thin adhesive layer are those typically used in commercial applications.

RESULTS

(i)   Thick Sample

Ultrasonic measurements were first carried out on the thick sample, initially at locations associated with the aluminium plate alone and then at locations across the bonded region interface. Results are shown in Figure 4, where (a)–(c) display ultrasonic waveforms obtained from the aluminium plate alone, and (d)–(f) reveal waveforms obtained across the bonded region.
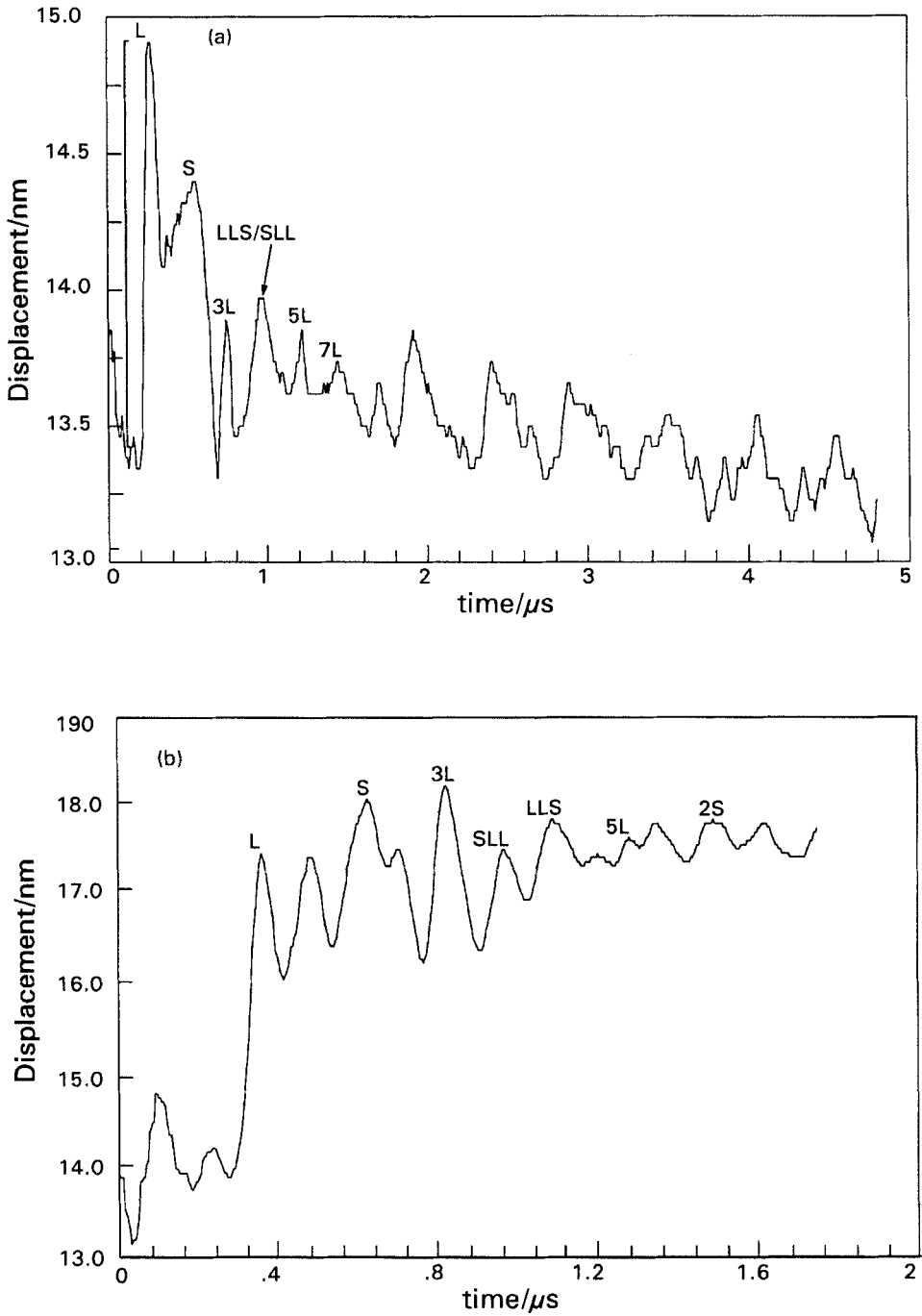
FIGURE 4   Through transmission ultrasonic waveforms obtained through a thick adhesive sample, aluminium plate alone (a)–(c), and the bonded region (d)–(f). Waveforms are presented on different timescales.
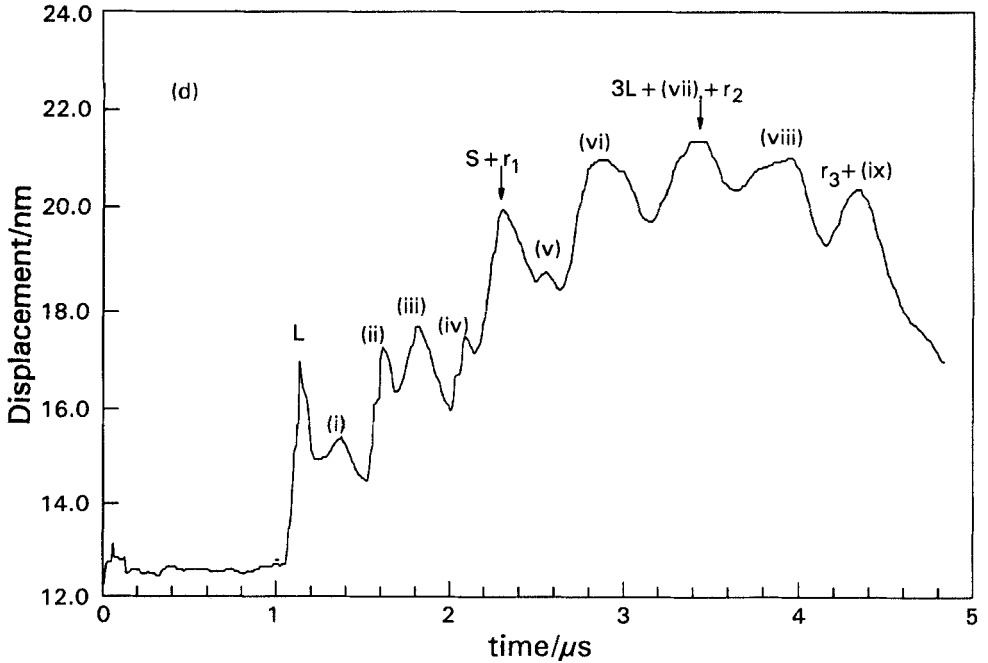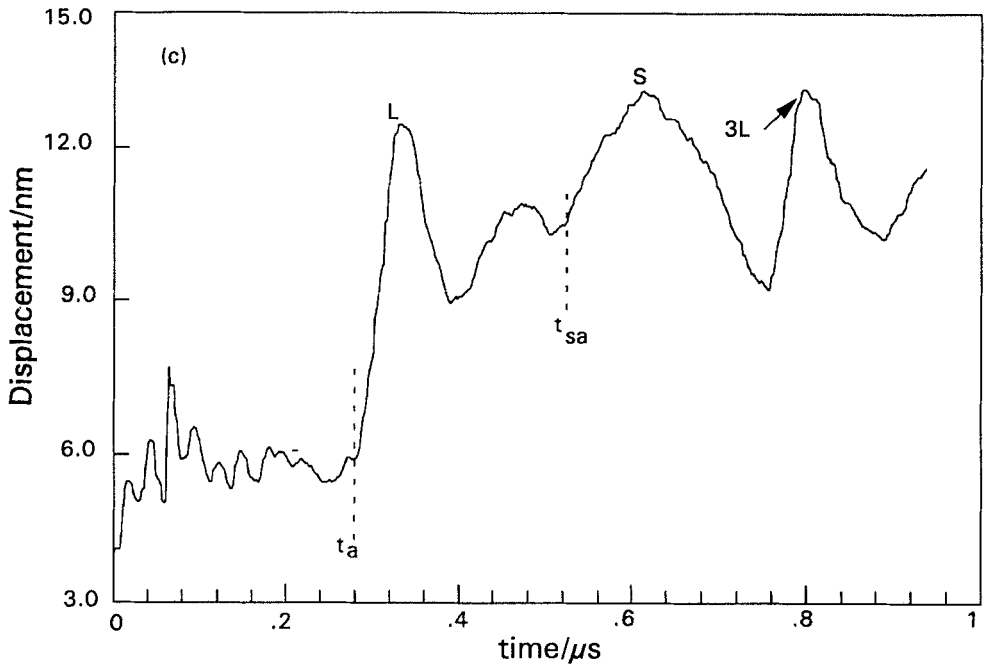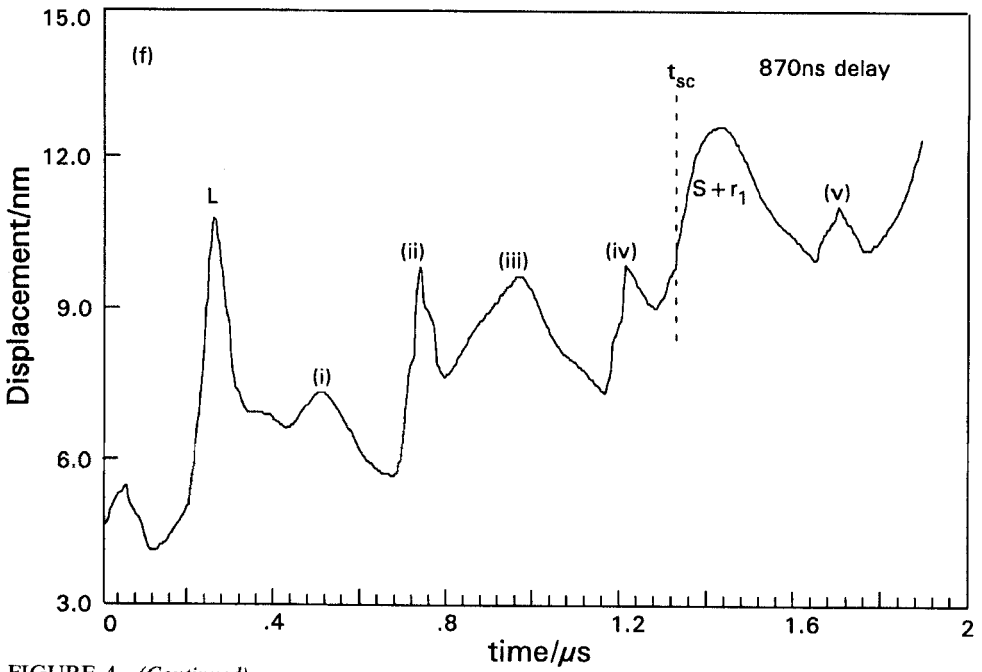
FIGURE 4   (Continued)
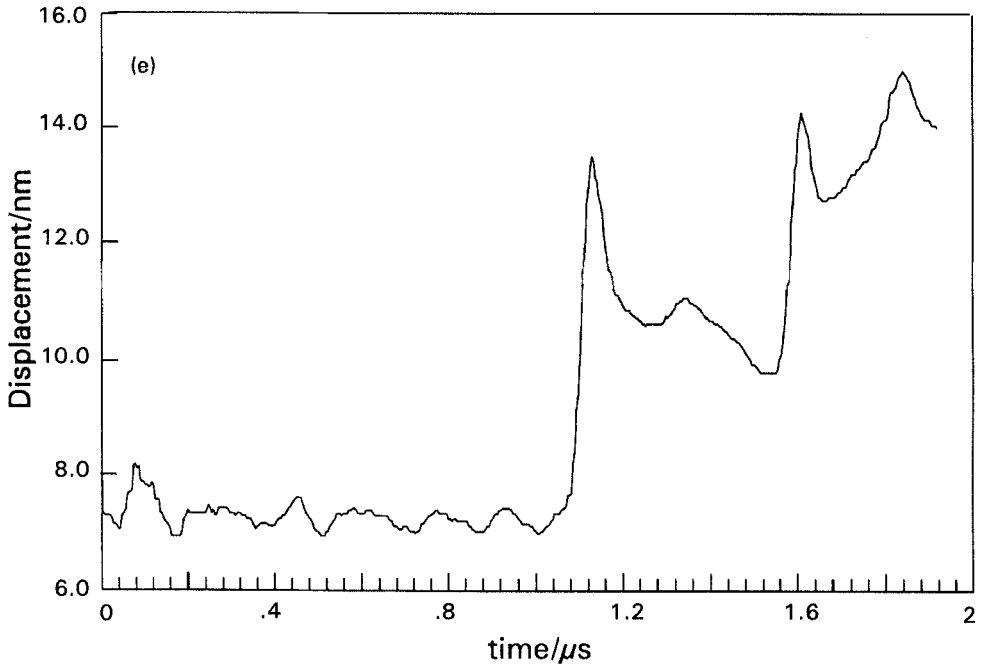
FIGURE 4   (Continued)

TABLE II

Calculated speeds of longitudinal waves in the aluminium plate and adhesive of the thick sample

Longitudinal wave in aluminium			Longitudinal wave in bonded region					
$t_a/\mu s$	a/mm	Speed a/t_a $mm\mu s^{-1}$	$t_c/\mu s$	$t_{la}/\mu s$ Calculated time in Al $(a+b)/c_1$	$t_d/\mu s$ $t_c - t_{la}$	d^*/mm	Speed d^*/t_d $mm\mu s^{-1}$
0.25 (± 0.01)	1.566	6.30 (± 0.02)	1.07 (± 0.02)	0.49	0.58	1.461	2.52 (± 0.13)

c_1 is the velocity of longitudinal waves in aluminium $= 6400$ m s^{-1}, t_a and t_c are the times spent within dimensions a and c of Figure 4.

From the waveforms of Figures 4(c) and (e), arrival times of longitudinal waves, from both the aluminium plate and the bonded region (t_a and t_d, respectively), were used to evaluate the speeds of the longitudinal waves in both the aluminium plate and the adhesive (Table II).

Time intervals spent by shear waves in the aluminium plate were calculated, using the dimensions a and b from Table I, and a shear-wave speed of 3150 m s^{-1} for aluminium.[21] From these, the time interval spent by shear waves in the adhesive was estimated, by using the shear arrival time, t_{sc}, through the bonded region, observed in the waveform of Figure 4(f). Results of the calculations are shown in Table III, together with the time intervals spent by longitudinal waves in the aluminium plate and adhesive. The time intervals of Table III were used to deduce possible configurations which may give rise to features evident in the waveforms of the bonded region; these configurations are represented in the schematic diagram of Figure 5.

Although mode conversions in through transmission are not predicted theoretically,[21] Figure 5(c) indicates that the peak labelled (i) in Figure 4(d)–(f) is due to a mode conversion, because the arrival time is too fast to be attributed to any other configuration. It may have been generated because of an unintentional offset of the optical axis formed by the detector/source lasers, which would cause the propagating wave to be detected at an angle and, therefore, to give rise to a degree of mode conversion;[21] alternatively, it may have been due to the fact that the ultrasonic wavefront is not a true plane wave at the boundary layers. Waveform peaks

TABLE III

Calculated time intervals spent by the longitudinal and shear waves in both the aluminium plate and the adhesive of the thick-jointed sample
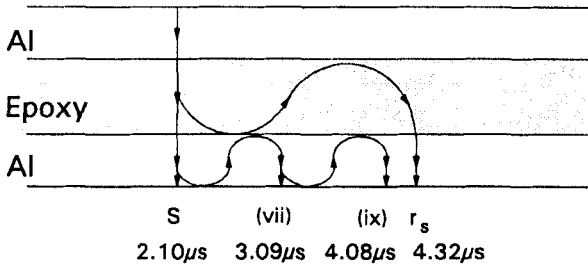
Longitudinal wave (from Table II)		Shear wave	
$t_{la}/\mu s$	$t_d/\mu s$	Calculated time in Al $(a+b)/c_2$ $t_{sa}/\mu s$	Time in adhesive/μs $t_{sc} - t_{sa}$
0.49	0.58	0.99	1.11 (± 0.02)

c_2 is the shear wave velocity in aluminium $= 3.15$ mmμs^{-1}.
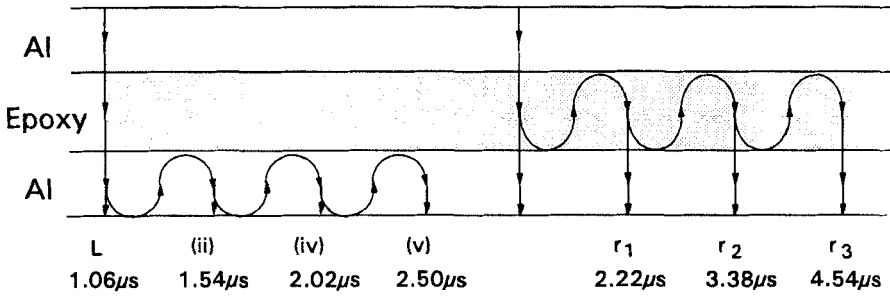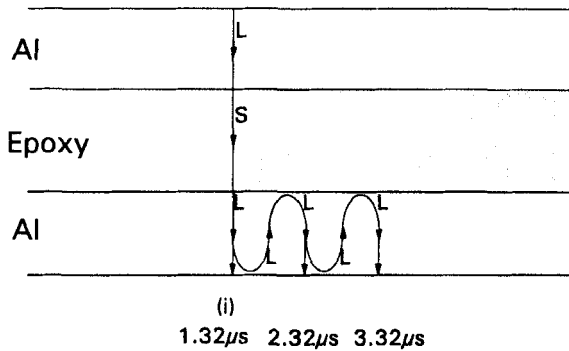
(a) Longitudinal Wave Arrival, L.

(b) Shear Wave Arrival, S.

(c) L and S Mode Conversion Arrival.

FIGURE 5   Possible configurations of ultrasonic propagation, giving rise to possible waveform features in a thick adhesive sample.

labelled (iii), (vi) and (viii) in Figures 4(d)–(f) have been attributed to sidewall echoes, which are caused by reflection from the adhesive-air boundary as shown in Figure 3.

In many cases overlap or convolutions occur which limit the resolution of pulses. For example, referring to Figure 5, similar arrival times of the following combinations are possible:

(a) Shear wave arrival, (S), with adhesive reverberation of longitudinal waves, (r_1);

(b) Aluminium reverberation, (vii), together with the second longitudinal arrival, (3L), and with adhesive reverberation, (r_2);

(c) Aluminium reverberation, (ix), together with adhesive reverberation, (r_3).

Using a thick sample, although reverberations within the aluminium plate were clearly visible from the L pulse observations, e.g. (ii), (iv) and (v), reverberations within the epoxy, r, were more difficult to detect. Example (a) shows that r_1 may have been convoluted with the shear wave arrival, and r_2 and r_3 may have undergone similar processes with other ultrasonic waves. Thus, time-domain analysis is complicated. Instead, some analysis in the frequency domain is described later.

(ii) Thin Samples

(a) Clean Sample   Examples of ultrasonic waveforms obtained from thin samples are shown in Figures 6(a)–(c). Using calculated time intervals displayed in Table III, features from the waveforms of Figures 6(a)–(c) arose from some wave configurations shown in Figure 7. Considering Figures 6(a)–(c), reverberations within the adhesive layer are clearly shown; reverberation times are shorter than those from thick samples.

The time spent by longitudinal waves in the adhesive layer was evaluated (Table IV) using the calculated value of speed in the adhesive, c_e, and the measured value of adhesive thickness, d^{**}, from Table I. Shear wave arrivals from the thin sample were not evident, because of complexity in the waveform. The time interval spent by shear waves in the thin adhesive layer, having thickness, d^*, were calculated by ratioing the time spent by the shear wave in the thick sample with the adhesive thickness, d^{**}; this produced the data recorded in Table V.

Figures 6(a)–(c) show that reverberations occurred at 80 ns intervals, consistent with a "round-trip" transit time derived from Table IV. Arrival times of this reverberation are shown in Figure 7(d). Figure 6(c) shows additional peaks, denoted by $*$, which cannot be identified. They are irregular, having time intervals ranging from

TABLE IV
Calculated time interval spent by longitudinal waves in the thin adhesive layer

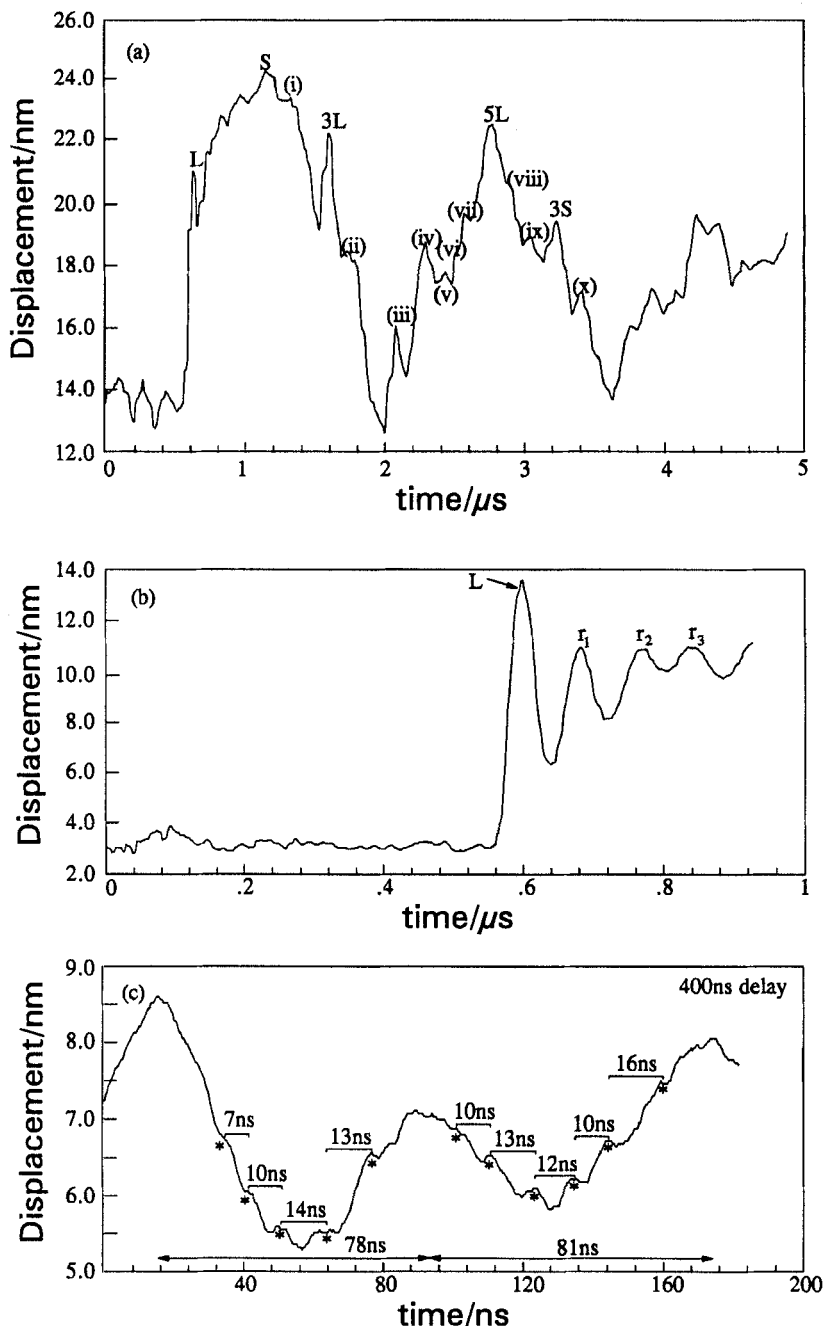| Longitudinal waves		
Epoxy thickness d^{**}/mm (Table 1)	c_e/mmμs^{-1} (Table II)	T_{ad}/μs d^{**}/c_e
0.102	2.52 ($\pm$0.15)	0.040

FIGURE 6   Waveforms obtained from measurements in a thin adhesive sample, having a bond line 0.102 mm thick. Waveforms (a)–(c) are presented on different timescales, with (b) showing reverberations of longitudinal pulses within the adhesive layer.
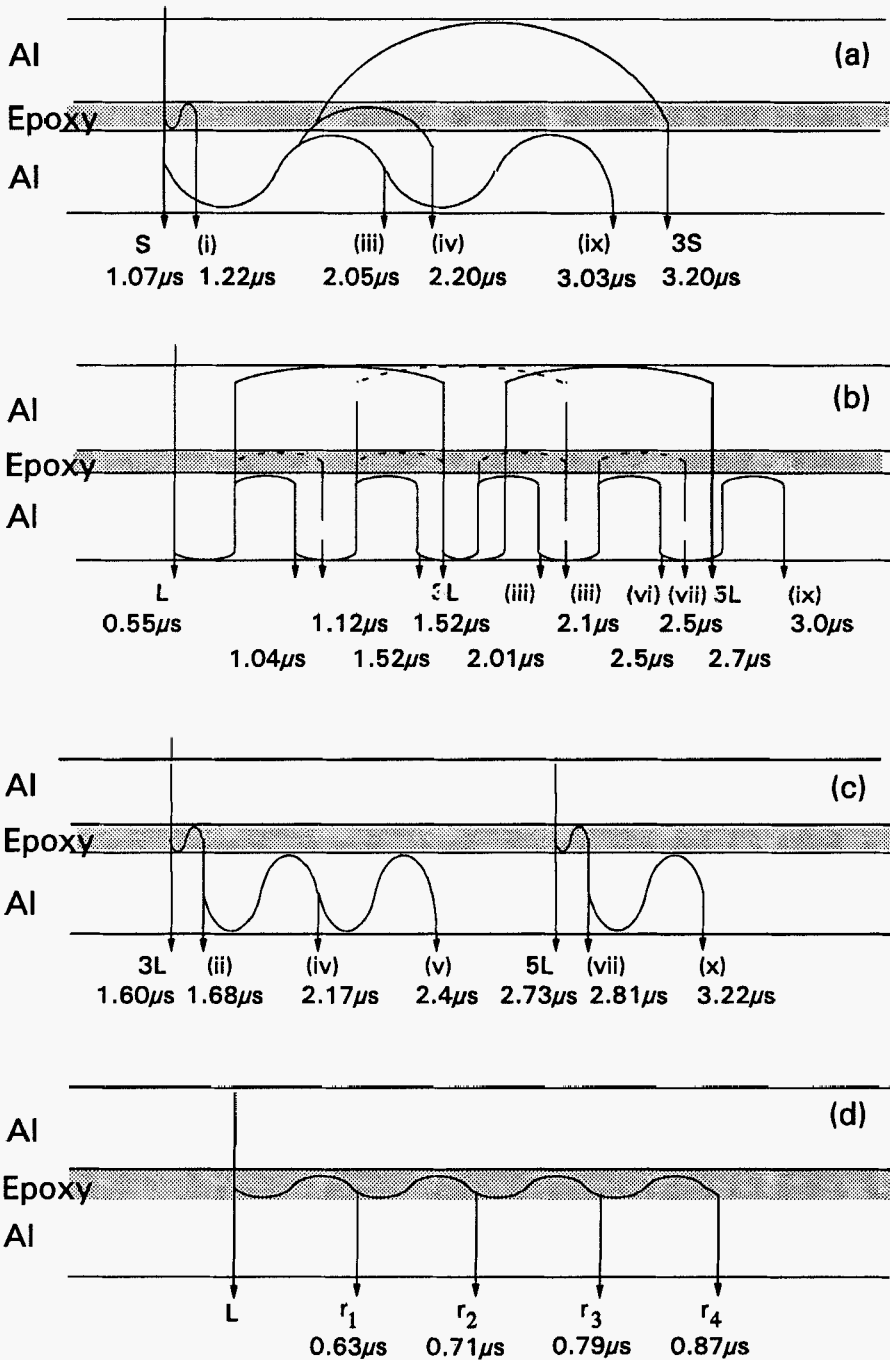
FIGURE 7   Possible configurations of ultrasonic propagation giving rise to waveform features observed in Figure 6: (a) shear wave interactions; (b) longitudinal wave interactions; (c) alternative longitudinal wave interactions; (d) longitudinal wave reverberation interactions, within the adhesive layer.

TABLE V
Calculated time interval spent by a shear wave in the thin adhesive layer

			Shear waves	
d^*/mm	d^{**}/mm	D d^{**}/d^*	Time in thick adhesive layer t_s/μs (from Table III)	Time in thin adhesive layer $T_{ad} = D x t_s$/μs
1.461	0.102	0.0698	1.11 ($\pm$0.02)	0.080

6–13 ns. Results presented above have been interpreted with the approximation that the oxide layer, characteristic of the pickling treatment in chromate/sulphuric acid, is vanishingly thin, and so merges into the adherend. Interestingly, these additional peaks may indicate the presence of the oxide layer.

Returning to longitudinal reverberation in the adhesive layer, Figure 6(b) clearly reveals the decrease in amplitude of successive signals. Figure 8(a) shows this interaction scheme where amplitudes of the successive peaks decrease as they suffer further reflections within the adhesive. In Figure 8(b), amplitudes are plotted against the number of reflections each configuration suffers in the adhesive layer. Assuming plane wave propagation, the following Equation may be derived from Figure 8(a):

$$A = A_o R^N \qquad (4)$$

A_o represents the amplitude of the first arrival, and is 39 mV, A represents the peak amplitude, R represents the reflection coefficient and N represents the number of reflections suffered by the wave in the adhesive layer. Experimental data showing the decrease in amplitude as a function of N are shown in Figure 8(b). Also shown in Figure 8(b) are three reflection coefficients, R, which have been fitted to the decay curve given by Equation (4). Using a value of R from adhesive to aluminium of 0.67, the closest fit to theory can be found. Hence, using Equation (2), the acoustic impedance of the adhesive, z_1, may be calculated as follows.

The impedance for aluminium, z_2, can be expressed

$$z_1 = z_2 - R_{12} (z_2 + z_1) \qquad (5)$$

$$\therefore z_2 = \frac{z_1 (1 + R_{12})}{(1 - R_{12})} \qquad (6)$$

Since for aluminium $c = 6400$ ms^{-1}, and $\rho = 2700$ kgm^{-3}

$$z_2 = c\rho = 17.28 \times 10^6 \text{ kgm}^{-2} \text{s}^{-1} \qquad (7)$$

Also from Figure 8, we may use $R_{12} = 0.67$; then substituting R_{12} and z_2 into Equation 6,

$$z_1 = 17.28 \times 10^6 \times \frac{(1 - 0.67)}{(1 + 0.67)} \text{ kgm}^{-2} \text{s}^{-1} \qquad (8)$$

The acoustic impedance of the adhesive is, therefore, 3.41×10^6 kgm^{-2} s^{-1}.
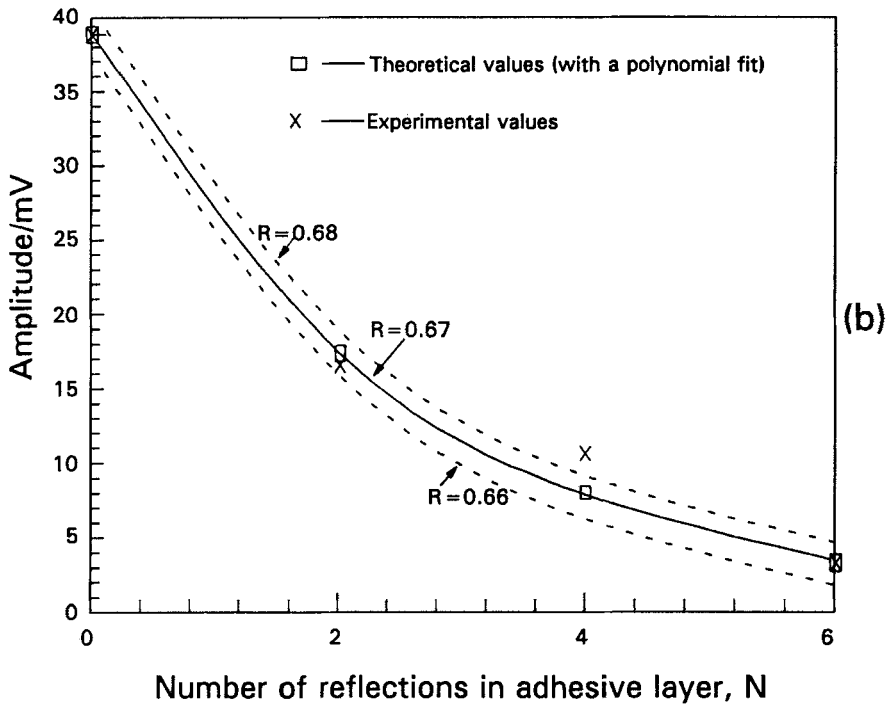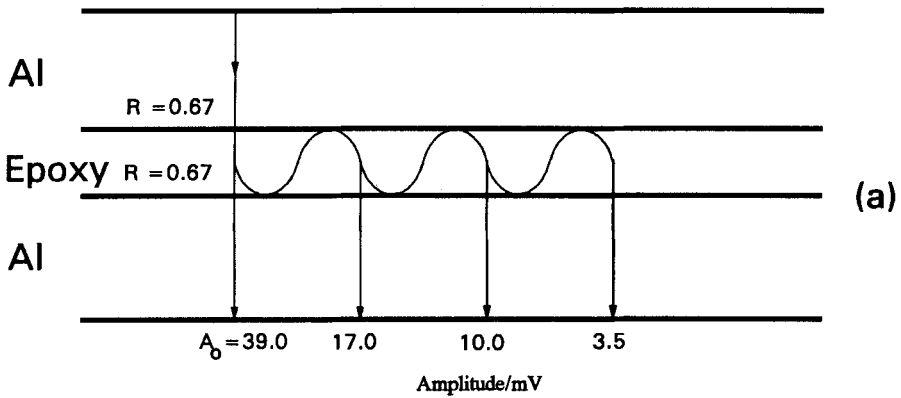
FIGURE 8 Ultrasonic behaviour arising from reverberation monitored in an aluminium-epoxy-aluminium interface: (a) Scheme showing the measured signal amplitude of reverberation, measured in mV, for successive reflections within the bond. Data were extracted from Figure 7(b), with a cross calibration of 1 nm≡2.83 mV. (b) Comparison of the experimental behaviour of reverberation amplitude for a number of ultrasonic reflections, N, with those predicted theoretically for reflection coefficients, R=0.66, R=0.67, and R=0.68.

However, from Equation (2),

$$z_1 = c_e \rho \tag{9}$$

where c_e is given in Table II: therefore, ρ, the density of the adhesive, has a value of 1350 (± 120) kgm^{-3}. For comparison, the swg density value for this adhesive is quoted as 1168 kgm^{-3} and, with a typical 2% shrinkage associated with curing, this will become 1192 kgm^{-3}. The swg density is obtained by a water displacement method, where the density is calculated from the weight of water displaced by the adhesive sample. In this present application, an ultrasound pulse travelled through the sample and, consequently, had intrinsic contact with a portion of adhesive material. It is this fundamental difference in the two measurement techniques which may give rise to slightly different density values. In practice, calibration may be necessary to correlate ultrasonic measurements with conventional approaches.

Thus, laser-ultrasound provides a means of calculating density from measurements of both successive reverberation amplitudes and the speed of the longitudinal pulse through the medium. In this way, it may be possible to assess changes in density on carrying out a scan across such an adhesive, thereby identifying regions of poor cure or perhaps the location of other defects.

(b) Comparison of Thin Sample, With and Without Oil Contamination Ultrasound measurements on thin samples, with and without oil contamination, are shown in Figures 9(a)–(d), over a 2 μs interval after laser pulse initiation. Their waveforms are clearly distinguishable. The oil-treated samples show reverberations, Figures 9(c)–(d), both within the adhesive (r) and within the aluminium plate on this timescale. The clean sample waveforms, Figures 9(a)–(b), display a strong shear arrival at 1.4 μs, which is significantly attenuated in the waveforms of the oil-contaminated samples. This may be explained by considering poor adhesion instead of total de-bonding,[11] based on vanishing tangential stresses at the interface. Such "smooth" boundary conditions are conceived as two solids separated by an inviscid liquid of infinitely small thickness, with an ability to transfer normal stresses, so that longitudinal waves are transferred effectively, whilst transverse waves (*i.e.* shear waves) are attenuated. Work by Pilarski and Rose,[11] using an oblique incidence technique, has revealed the higher sensitivity of transverse waves to interfacial weakness detection. They concluded that the advantage of shear waves in normal incidence was evident (since similar amplitude changes for longitudinal waves can only be expected for total de-bonding, *i.e.* reflection from a free surface). In a through-transmission configuration, the increase in any reflected shear wave amplitude in a poorly-bonded sample would be observed as an attenuation in shear wave content; this is consistent with ultrasonic waveforms shown in Figures 9(c)–(d), which were produced from measurements in oil-contaminated samples. It is noted here that the higher sensitivity of transverse waves in normal incidence has also been used for the detection of submicron gaps filled with liquid or gas.[22]

An oil-treated sample was further investigated by carrying out ultrasonic measurements at various positions along the bonded region, to identify particular areas of debond.[8] The data of Figure 10 were taken at successive positions, about 7 mm
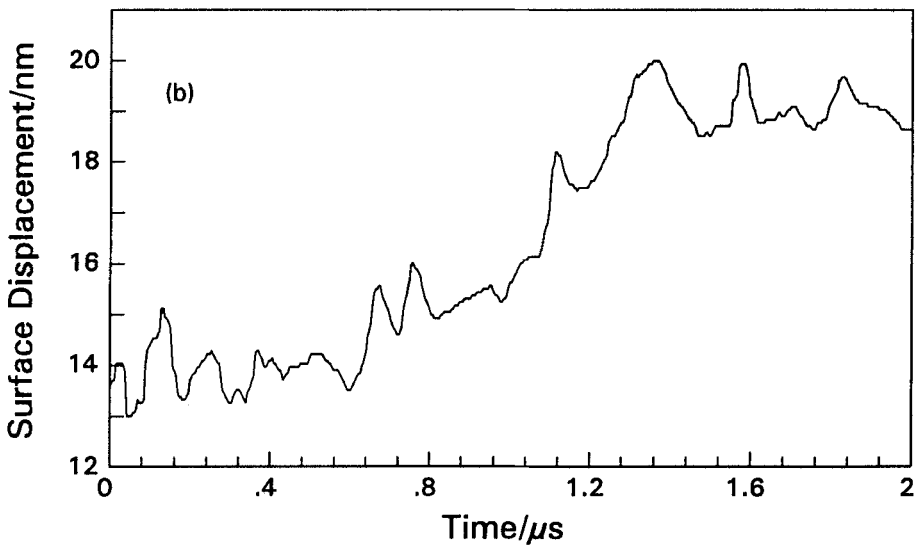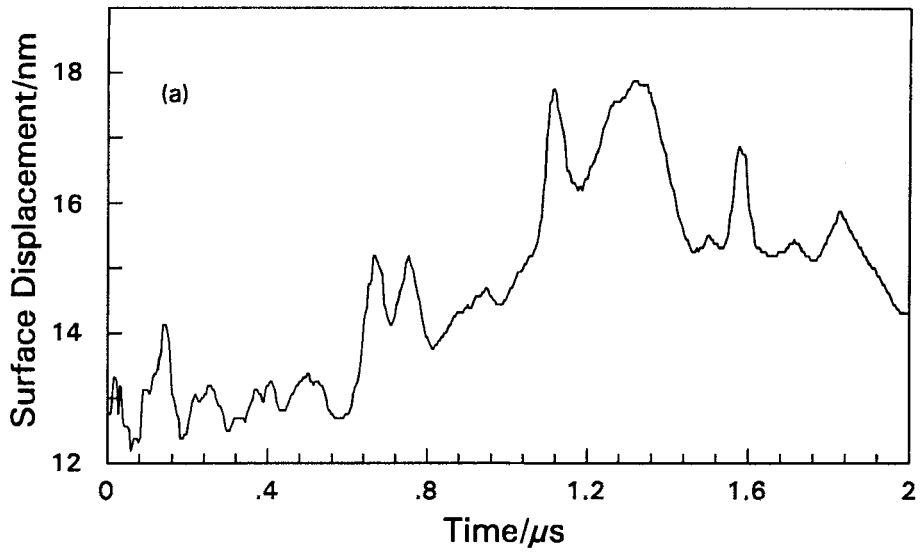
FIGURE 9   Comparison of waveforms from a thin adhesive sample in the absence, (a)–(b), and in the presence, (c)–(d), of oil contamination.
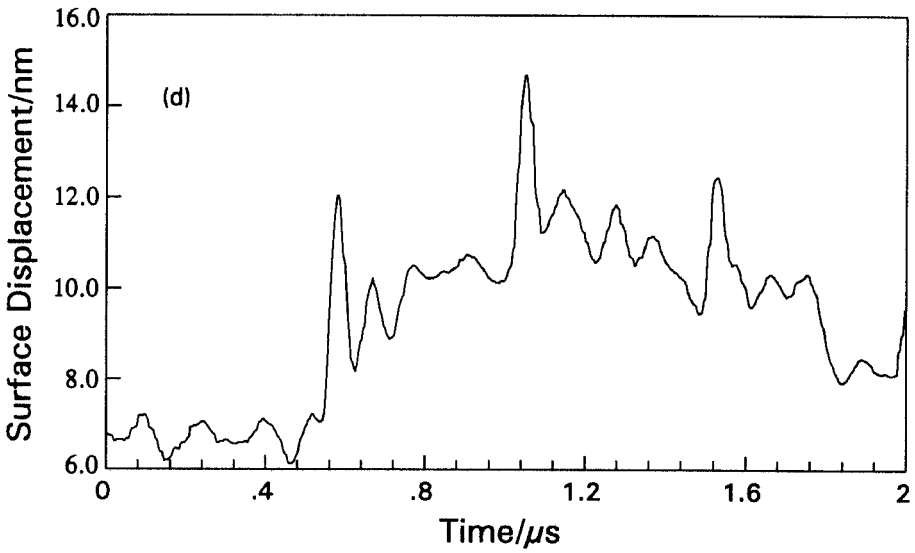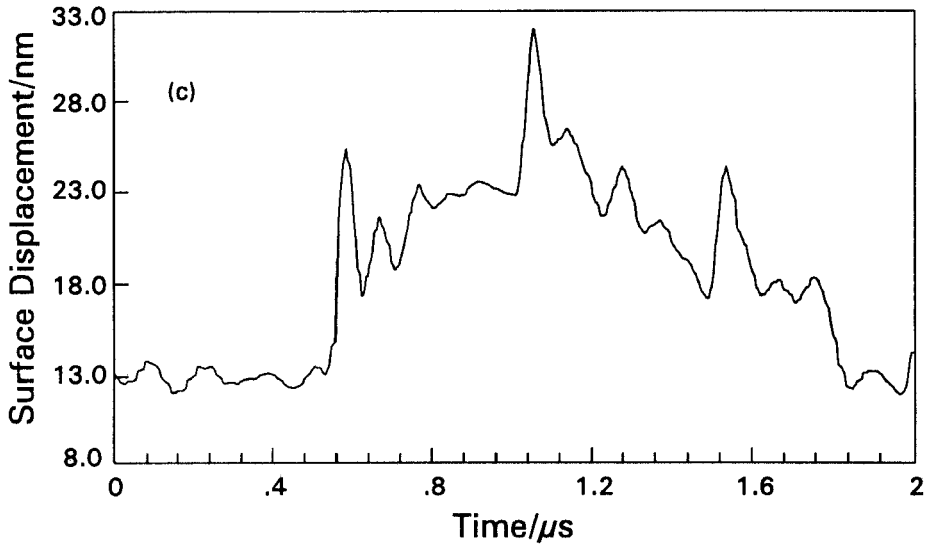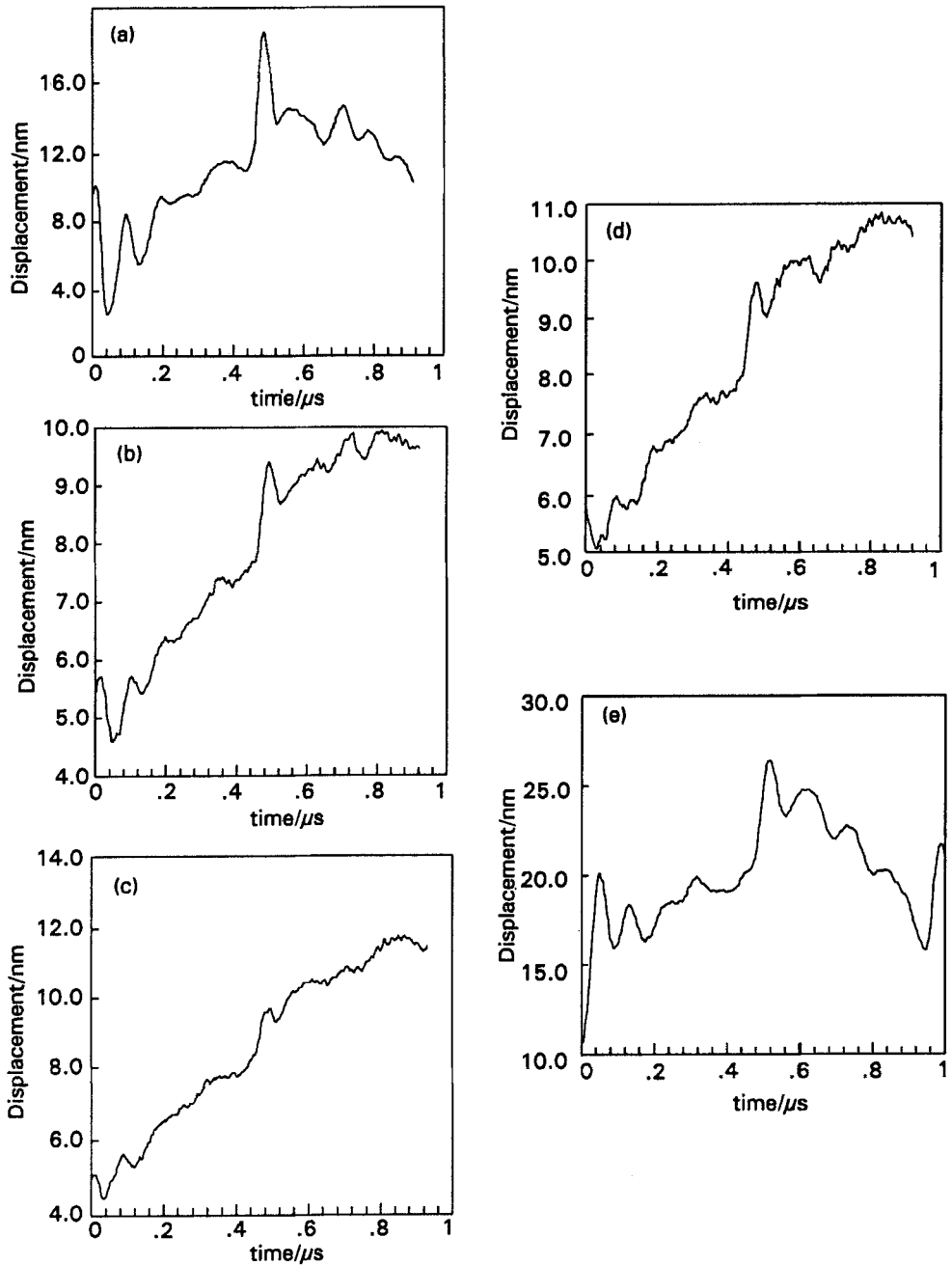
FIGURE 9   *(Continued)*

FIGURE 10 Waveforms obtained from an oil-contaminated sample with a thin (0.102 mm) adhesive layer, at progressive positions along its interface.

156	R. INCE, G. E. THOMPSON AND R. J. DEWHURST

apart, along the interface, where a sudden decrease in the ultrasonic displacement from (b)–(d) is observed, which suddenly increases again in Figure 10(e). Although variation in ultrasonic generation of the source may be a factor, waveform quality was consistent at each point. As a check, the laser was fired separately, 3 or 4 times per point, to examine consistency. Occasionally, at some sample positions, a complete loss of ultrasonic signal was observed over the first 2 μs interval, which may have been associated with an air pocket within the sample.

(iii)   Fast Fourier Transform Analysis

Fast Fourier Transforms (FFT's) were performed on several of the ultrasonic waveforms to assess any spectral changes arising from bond thickness variations or defects. Ultrasonic testing of adhesively-bonded joints in the frequency domain is known to be an effective method of testing for dis-bonds and bond thickness. This has been confirmed for the case of laser-generated ultrasound. Figure 11(a) is an FFT, corresponding to the Al plate alone and it has different features from FFT's produced from thick or thin samples, as shown in Figure 11(b) and Figure 12(a), respectively.

Figure 11(b) shows how the thick adhesive layer attenuates the aluminium plate frequencies, whereas the thin layer of Figure 12(a) still transmits these frequencies. Comparing Figure 11(b) and Figure 12(a), the fundamental frequency of the bonded region is seen to increase from 0.20 MHz in the thick layer to 0.60 MHz in the thin sample. No other significant visible frequency changes occurred, when the digitiser measured waveforms over a 5 μs timescale.

Additional features were measured when the digitiser operated over shorter timescales. For example, reverberation in a bonded aluminium plate with a thin bond line has already been presented in Figure 6(b). Its corresponding frequency spectrum is shown in Figure 12(b), where the dominant frequency occurred at 12.5 ± 0.5 MHz. The corresponding time of 80 ns is consistent with that expected for reverberation of longitudinal waves within the adhesive layer (see Table IV). The width of the resonant feature was the result of both signal processing effects and variation in thickness of the adhesive layer within the thin sample.

CONCLUSIONS

A laser/laser technique has employed ultrasonic pulses to propagate successfully through a lap joint in through-transmission measurements. This has made possible the measurement of the longitudinal velocity of ultrasound in the adhesive layer, which was calculated to be 2520 ± 130 m s^{-1}.

Possible ultrasonic interactions giving rise to ultrasonic waveform features within thick (1.46 mm) and thin (0.102 mm) samples have been suggested. Acoustic pulses reverberating within the thin adhesive layer were identified, which were clearly distinguishable from those within aluminium. Reverberation amplitudes within the adhesive layer of the thin sample were used to calculate a value for the density of the adhesive of 1350 (± 120) kgm^{-3}. This calculated value of density varied from
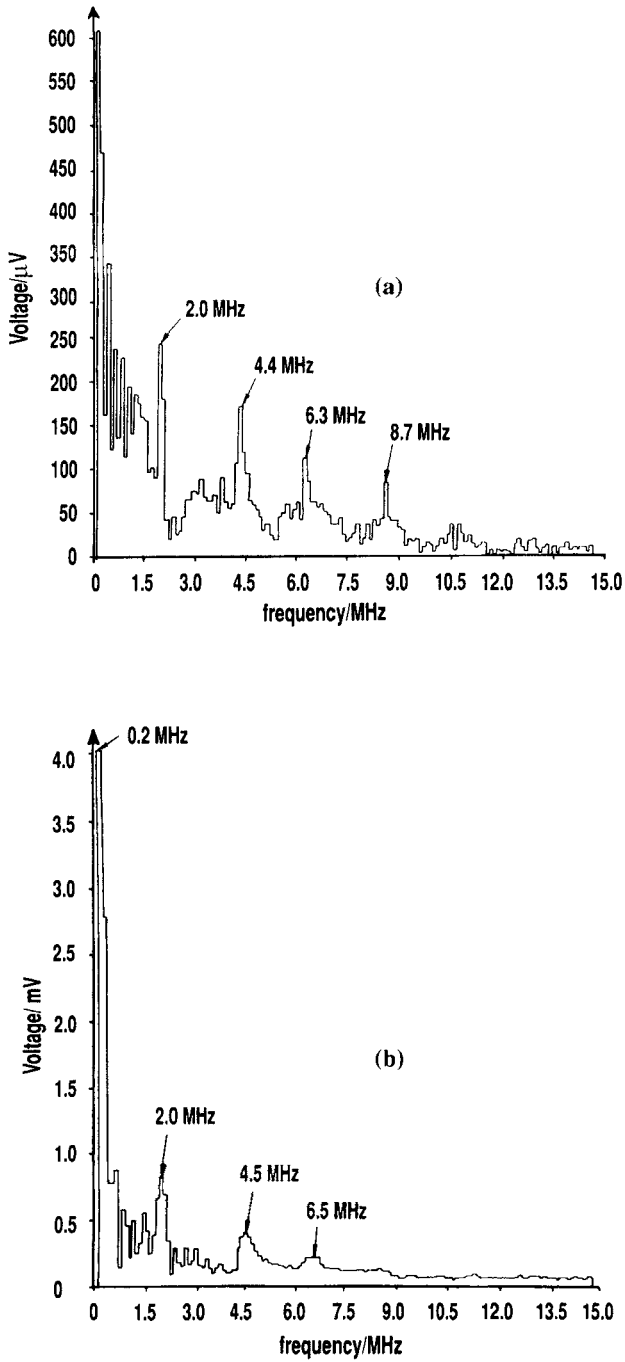
FIGURE 11   Fourier transform of time domain waveforms from a sample with a thick adhesive layer: (a) FFT of the aluminum plate; (b) FFT of the thick interface.
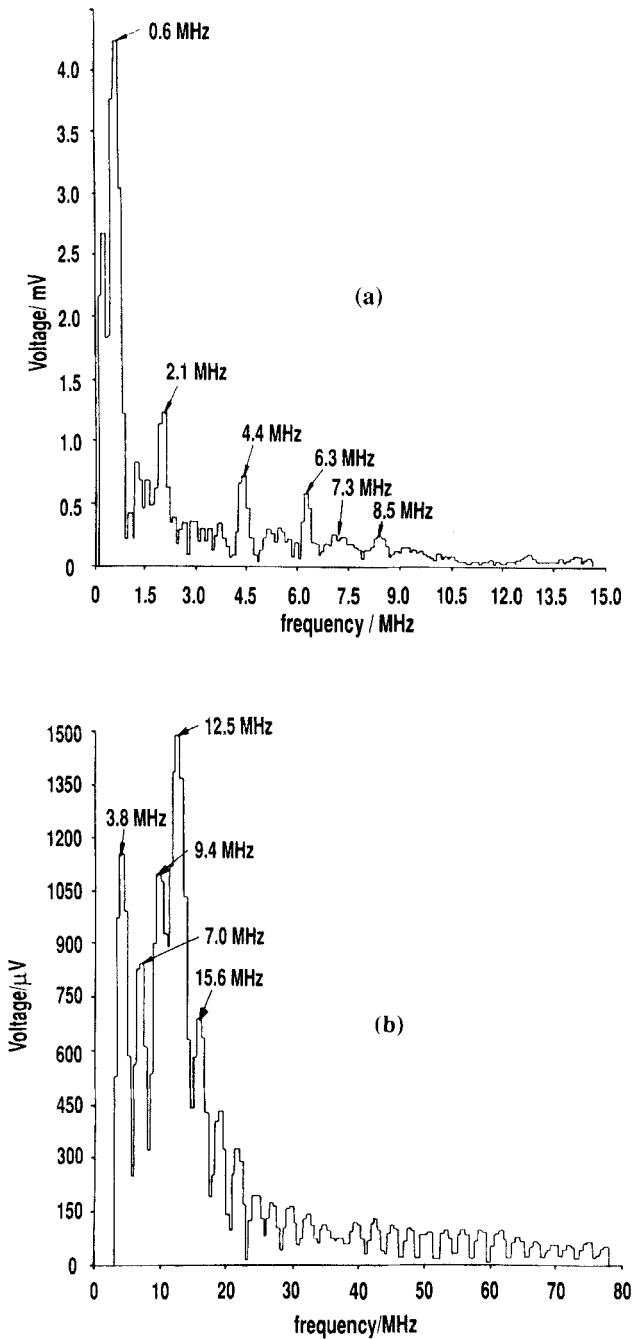
FIGURE 12 Fourier transform of time-domain waveforms from a sample with a thin adhesive layer: (a) FFT of the thin sample interface; (b) FFT of reverberations within the adhesive layer.

the expected swg density value of 1192 kgm^{-3}; discovery of the precise reasons for the difference between these two values is the purpose of future investigations.

Fast Fourier transforms of time-domain waveforms of the thick and thin samples were carried out, and a shift in a fundamental frequency of vibration from the thick to the thin sample was identified. In addition, the frequency of reverberation within the adhesive layer was identified as 12.5 MHz, consistent with calculations from time domain waveforms.

Acknowledgements

References

1. R. D. Adams, P. Cawley and C. C. H. Guyott, "Non-Destructive Inspection of Adhesively Bonded Joints," *J. Adhesion* **21**, 279–290 (1987).
2. P. Cawley, "The Impedance Method of Non-Destructive Inspection," *NDT International* **17**, 59 (1984).
3. R. D. Adams, P. Cawley, in *Research Techniques in NDT*, Vol. 8, R. S. Sharpe, Ed. (Academic Press, London and New York, 1985), pp. 303–360.
4. D. J. Hagemaier, "Bonded Honeycomb Structures-1," *NDT International* **4**, pp. 401–406, 1971.
5. D. J. Hagemaier, "Bonded Honeycomb Structures-2," *NDT International* **5**, pp. 38–48, 1972.
6. J. L. Rose, M. J. Avioli and R. Bilgram, "A Feasibility Study on the NDE of an Adhesively Bonded Metal to Metal Bond: An Ultrasonic Pulse-Echo Approach," *Brit. J. NDT* **25**, 67–71 (1983).
7. R. J. Schliekelmann, "NDT of Bonded Joints," *NDT International* **8**, pp. 100–110, 1975.
8. P. Cawley and R. D. Adams, "Defect Types and NDT Techniques for Composites and Bonded Joints," *Mat. Sci. and Techn.* **5**, 413–425 (1989).
9. C. M. Teller, K. J. Diercks, Y. BarCohen and A. K. Mal, "Recent Advances in the Application of Leaky Lamb Waves to the NDE of Adhesive Bonds," *J. Adhesion* **30**, 243–261 (1989).
10. L. M. Brekhovskikh, *Waves in Layered Media*, 2nd Edition (Academic Press, New York, 1980).
11. A. Pilarski and J. L. Rose, "Ultrasonic Oblique Incidence for Improved Sensitivity in Interface Weakness Determination," *NDT International* **21**, 241–246 (1988).
12. C. C. H. Guyott and P. Cawley, "Evaluation of the Cohesive Properties of Adhesive Joints Using Ultrasonic Spectroscopy," *NDT International* **21**, 233–240 (1988).
13. F. H. Chang, P. L. Flynn, D. E. Gordon and J. R. Bell, "Principles and Applications of Ultrasonic Spectroscopy in NDE of Adhesive Bonds," *IEEE Transactions on Sonics and Ultrasonics* **SU-23**, 334–338 (1976).
14. E. I. Madaras, W. P. Winfree, B. T. Smith and J. H. Heyman, "Detection of Bondline Delaminates in Multi-Layer Structures and Lossy Components," *Proc. IEEE Ultrasonics Symposium*, pp. 1047–1052, 1987.
15. D. Alleyne and P. Cawley, "A 2-Dimensional Fourier Transform Method for the Quantitative Measurement of Lamb Modes," *Proc. of the I.O.A.* **13**, 168–176 (1991).
16. J. B. Hoyes, Q. Shan and R. J. Dewhurst, "A Non-Contact Scanning System for Laser Ultrasonic Defect Imaging," *Meas. Sci. and Techn.* **2**, 628–634 (1991).
17. C. B. Scruby, R. L. Smith and B. C. Moss, "Microstructural Monitoring of Laser-Ultrasonic Attenuation and Forward Scattering," *NDT International* **19**, 307–313 (1986).
18. R. J. Dewhurst, C. Edwards, A. D. W. McKie and S. B. Palmer, "A Remote Laser System for Material Characterisation at High Temperatures," *Rev. of Prog. in Quantitative Non-Destructive Evaluation* **7B**, (Plenum Press, New York, 1988), pp. 1615–1622.
19. R. E. Corbett and R. J. Dewhurst, "Propagation of Laser-generated Acoustic Pulses in AGR Graphite," *Non-Destructive Testing and Evaluation* **5**, 121–134 (1990).
20. A. D. W. McKie, Ph.D. Thesis, University of Hull, 1987.
21. J. D. Achenbach, *Wave Propagation in Elastic Solids* (North-Holland Press, Amsterdam, 1980).
22. A. V. Clark and S. D. Hart, "Measurement of Ultrasound Reflected from Liquid Layers of Submicron Thickness," *Mat. Eval.* **40**, 866–873 (1982).